ACS Macro Letters

Letter

pubs.acs.org/macroletters

# Preparation of Composite Materials by Using Graphene Oxide as a Surfactant in Ab Initio Emulsion Polymerization Systems

Stuart C. Thickett and Per B. Zetterlund*

Centre for Advanced Macromolecular Design (CAMD), School of Chemical Engineering, The University of New South Wales, Sydney NSW 2052, Australia

Supporting Information

**ABSTRACT:** In this letter, we report a simple and unexpected method of producing polymer−graphene oxide (GO) composite materials via ab initio emulsion polymerization in water. On the basis of the recent reports concerning the surfactant-like behavior of GO for stabilizing oil-in-water emulsions, we prepared exfoliated GO sheets with lateral dimension approximately 200 nm for use as surfactant in the emulsion polymerization of styrene. We observed an expected "classic" surfactant behavior to produce stable nanoparticles at extremely low GO loadings (<0.1% w/w); however, at higher concentrations a highly aggregated, fibrous morphology was formed. This morphology is predominantly due to the electrolyte concentration (ionic strength) of the aqueous phase resulting in heterocoagulation of growing oligomers with dispersed GO sheets, which offers a convenient route toward preparing hybrid materials.

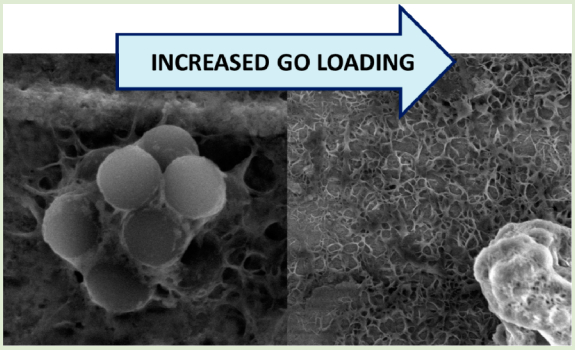


Graphene oxide (GO), the oxidized form of graphene prepared via the oxidation and exfoliation of bulk graphite, is often considered the most convenient material for the realization of graphene-based composite materials.[1] With respect to preparing functional polymeric materials, GO possesses numerous hydroxyl, epoxy, and carboxylate groups that permit polymeric functionalization and incorporation into a polymer matrix.[2−5] Of particular interest to our group is the recent report which describes the amphiphilic nature of GO,[6] whereby oil-in-water (o/w) emulsions are stabilized by adsorbed GO sheets at the oil−water interface (i.e., a Pickering emulsion).[7,8] This behavior, which is due to the ionizable carboxylate groups at the periphery and hydrophobic graphitic regions within the basal plane of GO, has given rise to its use as a colloidal stabilizer in heterogeneous polymerization, in particular miniemulsion polymerization.[9−12] The resultant materials, which in the case of recent work from our own group consist of polymer particles "armored" with a shell of GO,[11] represent a simple method to create hybrid materials.

The aim of this work was to demonstrate if GO could be used as a colloidal stabilizer in Pickering emulsion polymerization systems, as opposed to miniemulsion polymerization. This was recently achieved using Laponite clay discs as surfactant in the emulsion polymerization of various monomers[13] under appropriate conditions; other Pickering stabilizers successfully employed in emulsion polymerization include modified silica sols[14,15] and nanoparticles.[16,17] Emulsion polymerization has several technical advantages over miniemulsion polymerization, in particular the absence of a high shear emulsification step to create submicrometer-sized monomer droplets. To our knowledge, emulsion polymerization using GO as a surfactant has not been successfully achieved—however it has been incorrectly reported; previous reports claiming the preparation of polymer−GO hybrid materials by emulsion polymerization have used an ultrasonication step to create preformed submicrometer-sized monomer droplets[10,18] or droplet nucleation with an oil-soluble initiator,[19] which is inconsistent with the mechanism of emulsion polymerization[20,21] and more consistent with miniemulsion polymerization. In the case of a true emulsion polymerization, the locus of polymerization is either monomer-swollen micelles or newly nucleated particles formed via aqueous-phase initiation and propagation (as opposed to monomer droplet nucleation).

In this work, nanodimensional GO sheets were prepared by the oxidation of graphite nanofibers using a modified Hummers' method as reported previously.[11,22] These small sheets (Z-average hydrodynamic diameter 188 nm by dynamic light scattering (DLS), zeta potential = −48.4 mV in Milli-Q water) were dispersed in water via sonication and used as the aqueous phase for the ab initio emulsion polymerization of styrene for 24 h at 70 °C (target solids content 10% w/w, initiator (potassium persulfate) concentration ∼13 mM), which would be considered "typical" emulsion polymerization conditions.[23] At very low GO concentrations (<0.1% w/w relative to monomer), we observe that GO does behave as a surfactant; the average particle size decreases, and the particle

**Received:** June 3, 2013
**Accepted:** July 2, 2013
**Published:** July 5, 2013

   dx.doi.org/10.1021/mz400280t | ACS Macro Lett. 2013, 2, 630−634

**Table 1. Results of Ab Initio Emulsion Polymerizations of Styrene at Very Low GO Loadings (DLS Polydispersity Values in Brackets)**

| sample name | [GO] (mg mL$^{-1}$) | GO:styrene (%/w/w) | [KPS] (mM) | conversion after 24 h (%) | Z-average diameter (DLS, nm) | TEM/SEM diameter (nm) and observation | particle surface area (m$^2$ L$^{-1}$)[a] | GO surface area (m$^2$ L$^{-1}$)[b] |
|---|---|---|---|---|---|---|---|---|
| ST1 | 0 | 0 | 12.9 | 100 | 858 ± 14 (0.219) | 850 ± 29 (spheres) | 824 ± 84 | n/a |
| ST2 | 0.028 | 0.026 | 13.4 | 57.3 | 665 ± 20 (0.201) | 378 ± 26 (spheres) | 912 ± 192 | 12.6 |
| ST3 | 0.057 | 0.053 | 13.6 | 49.4 | 485 ± 10 (0.157) | 338 ± 20 (spheres) | 869 ± 160 | 25.7 |
| ST4 | 0.116 | 0.113 | 12.4 | 34.6 | 685 ± 51 (0.593) | 259 ± 24 (spheres, some fibres) | 782 ± 217 | 52.2 |

[a]Total particle surface area (m$^2$ L$^{-1}$) calculated from particle number $N_p$ (L$^{-1}$) and surface area of an individual particle (based on transmission electron microscopy (TEM) diameter). [b]Determined from product of experimental [GO] and half of GO surface area value of 900 m$^2$ g$^{-1}$ from ref 24.

number per unit volume ($N_p$) increases with increasing GO loading (Table 1 and Figure 1A). (At a GO loading of approximately 0.1% w/w relative to styrene, some large fibrous objects were observed by electron microscopy, which explains the difference between particle size as measured by DLS and scanning electron microscopy (SEM).) Electron microscopy images reveal polymer particles with roughened, textured surfaces, which may indicate the adsorption of GO sheets at the particle surface (Figure 1B). On the basis of a value of the surface area of GO of 900 m$^2$ g$^{-1}$,[24] we calculate that there is significantly more latex particle surface area than the area of GO sheets (see Table 1), indicating submonolayer particle surface coverage.

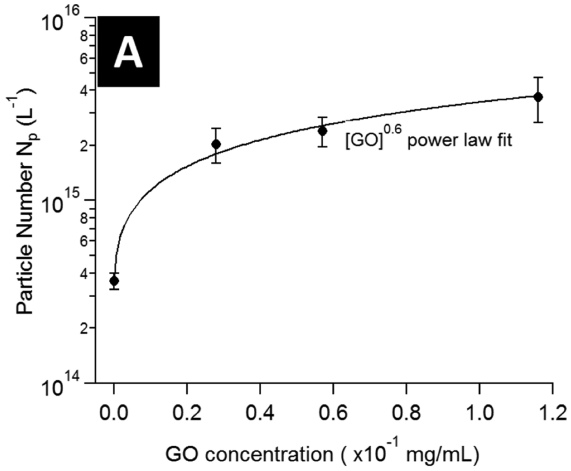


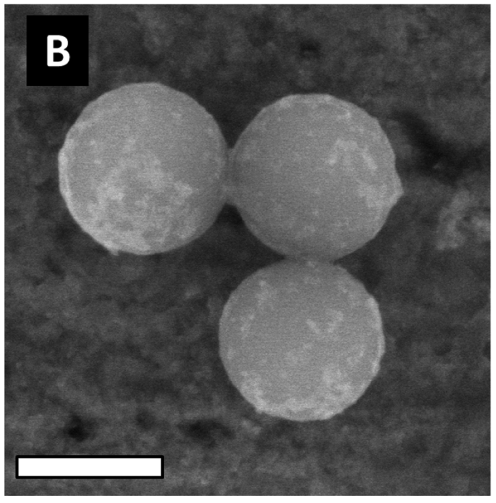


**Figure 1.** (A) Variation of particle number $N_p$ as a function of GO concentration. (B) SEM image of polystyrene particles from experiment ST4 (0.1% GO w/w relative to styrene), displaying a patchy surface (scale bar = 200 nm).

Data shown in Figure 1A show that this system strongly follows the classic "Smith–Ewart" expectation that $N_p$ is proportional to [surfactant]$^{0.6}$ based on the TEM diameters (Table 1).[25] This result is further vindication of the surfactant-like properties of GO, which has previously been demonstrated by interfacial tension measurements and the ability to stabilize o/w emulsions.[6,7] The exact nucleation mechanism in these systems remains to be clarified; however, it is clear that GO does behave as a surfactant in the sense that an increase in the GO concentration leads to an increase in the number of particles. For completeness, we acknowledge that satisfying a particular power law does not verify the particle formation mechanism in this system: the 0.6 power law present in the Smith–Ewart model is based on the assumption that particle formation ceases when micelles disappear; however, there are no micelles present in this system. The 0.6 power dependency is also predicted by homogeneous nucleation,[26] whereas Fitch[27] and Gardon[28,29] have experimentally demonstrated different power law exponents. We also note that GO also behaves as an inhibitor in these systems as evident from much reduced conversion of monomer to polymer; this is consistent with previous work in our group[11] and also with the inherent structure of GO, which possesses a high concentration of phenolic hydroxyl groups (similar to many polymerization inhibitors, such as *tert*-butylcatechol).

When polymerization was performed at higher GO loadings (see Supporting Information for experiment details), we observed a quite unexpected change in the final latex and resultant particle morphology. At all GO loadings between 0.5 and 5% w/w relative to styrene, the milky brown latex (the color being due to the GO present in the system) rapidly settled upon standing (Figures 2A and 2B), leaving a clear supernatant. The final conversion after 24 h was low at all GO concentrations studied (as low as 17% when the GO concentration was 5% w/w relative to styrene), indicative of the inhibitory nature of GO. Electron microscopy analysis revealed the existence of numerous multimicrometer aggregates and fiber-like materials (Figures 2C and 2D), moving away from the discrete spherical particles observed at low GO concentrations (Table 1) discussed earlier.

All samples with a GO loading lower than 1% w/w were soluble in chloroform and subsequently purified via precipitation into methanol (N.B. GO can be dispersed into methanol, and some free GO may be lost during purification; the product was insoluble in chloroform at higher GO loadings). The material formed was a pale brown powder (see Supporting Information) that was characterized by FTIR spectroscopy; in addition to typical polystyrene peaks, very


dx.doi.org/10.1021/mz400280t | ACS Macro Lett. 2013, 2, 630–634

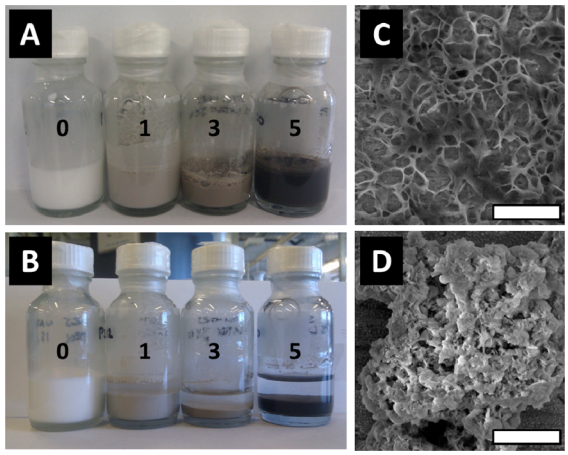


**Figure 2.** Polystyrene latexes prepared by ab initio emulsion polymerization containing 0, 1, 3, and 5% w/w GO relative to monomer (ST1, ST6, ST7, and ST8) both (A) immediately after synthesis and (B) upon standing overnight. (C) SEM image from sample ST6, 1% w/w GO loading (scale bar = 1 $\mu$m). (D) SEM image from sample ST8, 5% w/w GO loading (scale bar = 2 $\mu$m).

strong characteristic adsorptions were present at 1220, 1360, and 1720 $cm^{-1}$, indicative of specific vibrations related to GO, namely, C−OH stretching vibrations, tertiary hydroxyl deformations, and ketone/carboxylate vibrations, respectively.[30−32] The products were soluble in DMF, ethyl acetate, and toluene but only partially soluble in THF and insoluble in cyclohexane and acetone (all good solvents for pure polystyrene), indicating the formation of a hybrid material. Sonication of the product in water produced no free GO, suggesting either covalent attachment of the polymer to GO and/or physical entanglement and entrapment within the polymer matrix.

We rationalize this unusual emulsion behavior partially on the basis of instability of GO nanosheets dispersed in water at high electrolyte concentration (i.e., high ionic strength). At a fixed GO concentration of 0.1 mg $mL^{-1}$, we observe by light scattering and zeta potential measurements that GO sheets begin to aggregate and settle out of solution at an ionic strength of approximately 40−60 mM (using NaCl as a 1:1 electrolyte) (Figure 3). In the case of ab initio emulsion polymerization, the initiator (potassium persulfate) is also a 2:1 electrolyte and hence affects the stability of the GO "surfactant" in our

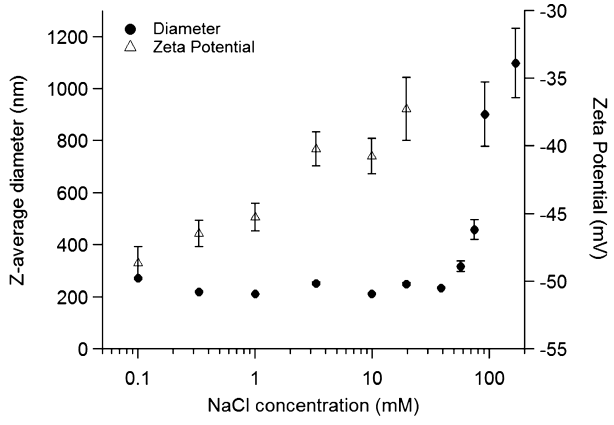


**Figure 3.** Z-average diameter and zeta potential of GO (0.1 mg $mL^{-1}$ in water) as a function of NaCl concentration (mM).

experiments. In our emulsion polymerization experiments, the chosen initiator concentration of 13 mM equates to an ionic strength of 40 mM, which represents conditions close to the upper limit of GO stability at this GO concentration. In a separate experiment, the stability of aqueous GO dispersions was monitored visually at the same fixed ionic strength (i.e., 40 mM, based on 13 mM potassium persulfate) but at different GO concentrations (ranging from 0.1 to 1 mg $mL^{-1}$ in water). We observe aggregation and settling at all GO concentrations where unstable latexes were formed (see Supporting Information), indicating that only extremely dilute GO dispersions (such as those in Table 1) remain stable at this (high) fixed ionic strength, possibly due to reduced frequency of collisions between GO sheets in solution. Under emulsion polymerization conditions, an unstable dispersion of GO may behave as a type of flocculant (via either a depletion or bridging mechanism)[33,34] resulting in the rapid settling of the resultant latexes observed in Figure 2.

To further test the importance of the ionic strength of the aqueous phase, an ab initio emulsion polymerization was performed at 1% w/w GO (relative to styrene) using a 5-fold reduction in initiator concentration (to reduce the ionic strength of the aqueous phase). In this instance a milky brown latex was not formed, but a clear, dark brown solution similar to the starting GO dispersion remained after polymerization for 24 h to reach 19% conversion. The appearance of the emulsion indicates that a significant portion of the GO sheets remains dispersed in the continuous phase as opposed to being adsorbed at the particle surface. TEM analysis revealed the presence of small polymer particles of 110 nm diameter, as opposed to the multimicrometer aggregates formed at the higher initiator concentration using this GO loading as described earlier (Figure 4). Identical behavior is observed

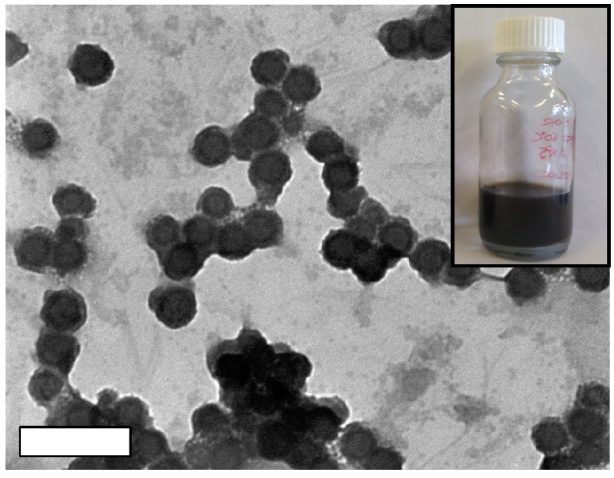

**Figure 4.** TEM image of latex produced from emulsion polymerization of styrene in the presence of GO (1% w/w relative to monomer) at low initiator concentration ([KPS] = 2 mM). The resultant latex (inset) is dark brown and semitransparent (scale bar = 300 nm).

when polymerization is performed using ACVA (although only 0.4% conversion in 24 h), an aqueous phase initiator that is a weak acid and so contributes minimally to the ionic strength of the aqueous phase (see Supporting Information). At a low persulfate concentration but in the presence of added NaCl (35.9 mM NaCl; total ionic strength 44.9 mM), a milky brown latex which settles upon standing is formed (81% conversion in


dx.doi.org/10.1021/mz400280t | ACS Macro Lett. 2013, 2, 630−634

24 h), and a highly aggregated morphology is once again observed.

We interpret the above results in terms of the homogeneous coagulation mechanism of particle formation in emulsion polymerization.[35] At low ionic strengths, GO has a large negative zeta potential and increased tendency to remain dispersed in the aqueous phase. The likelihood of GO sheets adsorbing at a particle interface as a surfactant is hence reduced. Under these conditions, polymer nanoparticles nucleate and grow via homogeneous nucleation; GO in the aqueous phase acts as an aqueous phase inhibitor and to a minor extent as a surfactant. At elevated ionic strength, the surfactant-like properties of GO are increased (due to a less negative zeta potential), but colloidal stability of GO in the aqueous phase is diminished. As a result, it behaves as an unstable "precursor particle", with the possibility of heterocoagulation between a GO sheet and growing oligomers that are insoluble in the aqueous phase (analogous to the particle formation proposed by Sheibat-Othman et al.[17]). The combination of increased surface activity at high ionic strength yields small, stable nanoparticles at low GO concentrations (Table 1), but limited colloidal stability and potential heterocoagulation at higher GO loadings give rise to ill-defined morphologies. It follows that efficient surfactant-like behavior of GO is only expected under conditions where the ionic strength is low enough to allow sufficient dispersibility of GO in water but high enough to provide a sufficient driving force for GO sheets to migrate to the particle interface.

In conclusion, we report for the first time evidence of the surfactant-like properties of GO in ab initio emulsion polymerization systems which are most readily evident at low GO loadings. A more intriguing result occurs at higher GO loadings, whereby simply changing the ionic strength of the aqueous phase (via an initiator or inert electrolyte) provides control over the final particle morphology, ranging from discrete polymer particles through to GO−polymer aggregates. The simplicity of emulsion polymerization makes this approach a potentially attractive method for the creation of hybrid materials on a large scale.

## EXPERIMENTAL SECTION

**Materials.** Styrene (99%, Sigma Aldrich) was purified by passing through a column of activated basic alumina (Ajax) to remove inhibitor. Potassium persulfate (KPS, Sigma) and 4,4′-azobis(cynovaleric acid) (ACVA, Sigma) were used as received. GO was prepared from graphite nanofibers (Catalytic Materials LLC) with an average cross-sectional diameter of 100 nm based on a modified Hummers' method as reported previously.[11] GO was dispersed into Milli-Q water via ultrasonication (Branson Digital Sonifier 450) at 50% amplitude while on ice for 2 min. Water used in all emulsion polymerization experiments was Milli-Q grade.

**Emulsion Polymerization Experiments.** The target solid content for all emulsion polymerizations was 10% w/w (1 g of monomer; 10 g of total emulsion). In a typical emulsion polymerization experiment, the aqueous phase (8 mL of total volume, consisting of GO dispersed in water at the desired concentration) was added to a round-bottom flask, sealed with a rubber septa, and degassed under magnetic stirring. Styrene (1 g) was added via syringe; degassing continued for 15 min while the mixture was emulsified. The vessel was then lowered into a temperature-controlled oil bath, after which an aqueous solution of KPS (approximately 33 mg in 1 mL of water) was injected to commence polymerization. Polymerization was allowed to proceed for 24 h. Conversion was determined by gravimetry.

**Characterization Techniques.** Transmission electron micrographs (TEM) were obtained using a JEOL1400 Transmission Electron Microscope at an accelerating voltage of 100 kV. SEM images were recorded on a Hitachi S-900 SEM at a working distance of approximately 5 mm and an accelerating voltage of 4 kV.

X-ray photoelectron spectroscopy (XPS) was performed using a Kratos Axis ULTRA XPS with hemispherical electron energy analyzer. The incident radiation was monochromatic A1 X-rays (1486.6 eV) at 225 W (15 kV, 15 mA). Survey scans were taken at an analyzer pass energy of 160 eV, over a range of 0−1360 eV (1 eV increments, dwell time 100 ms). High-resolution scans were also recorded (0.2 eV increments, 250 ms dwell time).

Fourier transform infrared (FTIR) spectra were obtained using a Bruker IFS66/S instrument in attenuated total reflectance (ATR) mode. A minimum of 128 scans were recorded, acquired between 500 and 4000 $cm^{-1}$ at a resolution of 4 $cm^{-1}$.

Z-average particle size and zeta-potential measurements were recorded using a Malvern ZetaSizer NanoSeries, operating a 4 mW HeNe laser at 633 nm at a scattering angle of 173°. All reported results are based on the average of five measurements.

## ASSOCIATED CONTENT

### Supporting Information

GO characterization including XPS and FTIR spectra, further TEM and SEM images of polymer nanoparticles, digital photographs of GO solutions, and characterization of polymeric products. This material is available free of charge via the Internet at http://pubs.acs.org.

## AUTHOR INFORMATION

### Corresponding Author

*E-mail: p.zetterlund@unsw.edu.au. Phone: +61-2-9385-4331.

### Notes

The authors declare no competing financial interest.

## ACKNOWLEDGMENTS

Stuart Thickett gratefully acknowledges the provision of a Vice-Chancellor's Post-Doctoral Research Fellowship from The University of New South Wales.

## REFERENCES

(1) Compton, O. C.; Nguyen, S. T. *Small* **2010**, *6*, 711.
(2) Kim, H.; Abdala, A. A.; Macosko, C. W. *Macromolecules* **2010**, *43*, 6515.
(3) Salavagione, H. J.; Martinez, G.; Ellis, G. *Macromol. Rapid Commun.* **2011**, *32*, 1771.
(4) Badri, A.; Whittaker, M. R.; Zetterlund, P. B. *J. Polym. Sci., Part A: Polym. Chem.* **2012**, *50*, 2981.
(5) Thickett, S. C.; Zetterlund, P. B. *Curr. Org. Chem.* **2013**, *17*, 956.
(6) Kim, J.; Cote, L. J.; Kim, F.; Yuan, W.; Shull, K. R.; Huang, J. *J. Am. Chem. Soc.* **2010**, *132*, 8180.
(7) Cote, L. J.; Kim, J.; Tung, V. C.; Luo, J.; Kim, F.; Huang, J. *Pure Appl. Chem.* **2011**, *83*, 95.
(8) Kim, J.; Cote, L. J.; Huang, J. *Acc. Chem. Res.* **2012**, *45*, 1356.
(9) Etmimi, H. M.; Tonge, M. P.; Sanderson, R. D. *J. Polym. Sci., Part A: Polym. Chem.* **2011**, *49*, 1621.
(10) Song, X.; Yang, Y.; Liu, J.; Zhao, H. *Langmuir* **2010**, *27*, 1186.

(11) Che Man, S. H.; Thickett, S. C.; Whittaker, M. R.; Zetterlund, P. B. *J. Polym. Sci., Part A: Polym. Chem.* **2013**, *51*, 47.
(12) Etmimi, H. M.; Sanderson, R. D. *Macromolecules* **2011**, *44*, 8504.
(13) Teixeira, R. F. A.; McKenzie, H. S.; Boyd, A. A.; Bon, S. A. F. *Macromolecules* **2011**, *44*, 7415.
(14) Sacanna, S.; Kegel, W. K.; Philipse, A. P. *Phys. Rev. Lett.* **2007**, *98*, 158301.
(15) Schmid, A.; Tonnar, J.; Armes, S. P. *Adv. Mater.* **2008**, *20*, 3331.
(16) Colver, P. J.; Colard, C. A. L.; Bon, S. A. F. *J. Am. Chem. Soc.* **2008**, *130*, 16850.
(17) Sheibat-Othman, N.; Bourgeat-Lami, E. *Langmuir* **2009**, *25*, 10121.
(18) Gudarzi, M. M.; Sharif, F. *Soft Matter* **2011**, *7*, 3432.
(19) Yin, G.; Zheng, Z.; Wang, H.; Du, Q.; Zhang, H. *J. Colloid Interface Sci.* **2013**, *394*, 192.
(20) Gilbert, R. G. *Emulsion Polymerisation: A Mechanistic Approach*; Academic Press: San Diego, 1995.
(21) Thickett, S. C.; Gilbert, R. G. *Polymer* **2007**, *48*, 6965.
(22) Luo, J.; Cote, L. J.; Tung, V. C.; Tan, A. T. L.; Goins, P. E.; Wu, J.; Huang, J. *J. Am. Chem. Soc.* **2010**, *132*, 17667.
(23) Goodwin, J. W.; Hearn, J.; Ho, C. C.; Ottewill, R. H. *Colloid Polym. Sci.* **1974**, *252*, 464.
(24) Dreyer, D. R.; Park, S.; Bielawski, C. W.; Ruoff, R. S. *Chem. Soc. Rev.* **2010**, *39*, 228.
(25) Smith, W. V.; Ewart, R. H. *J. Chem. Phys.* **1948**, *16*, 592.
(26) Roe, C. P. *Ind. Eng. Chem.* **1968**, *60*, 20.
(27) Fitch, R. M. *Br. Polym. J.* **1973**, *5*, 467.
(28) Gardon, J. L. *J. Polym. Sci., Part A: Polym. Chem.* **1968**, *6*, 643.
(29) Gardon, J. L. *J. Polym. Sci., Part A: Polym. Chem.* **1968**, *6*, 687.
(30) Stankovich, S.; Piner, R. D.; Nguyen, S. T.; Ruoff, R. S. *Carbon* **2006**, *44*, 3342.
(31) Kaminska, I.; Das, M. R.; Coffinier, Y.; Niedziolka-Jonsson, J.; Sobczak, J.; Woisel, P.; Lyskawa, J.; Opallo, M.; Boukherroub, R.; Szunerits, S. *ACS Appl. Mater. Interfaces* **2012**, *4*, 1016.
(32) Szabó, T.; Berkesi, O.; Dékány, I. *Carbon* **2005**, *43*, 3186.
(33) Jenkins, P.; Snowden, M. *Adv. Colloid Interface Sci.* **1996**, *68*, 57.
(34) Fellows, C. M.; Doherty, W. O. S. *Macromol. Symp.* **2005**, *231*, 1.
(35) Priest, W. J. *J. Phys. Chem.* **1952**, *56*, 1077.